Proposal for a Cosmic Ray Veto Shield for the MINOS Far Detector

The MINOS collaboration

June 1, 2002

Abstract

The MINOS far detector offers a unique opportunity to measure whether atmospheric anti-neutrinos oscillate in the same way as neutrinos. Recently, enough of the far detector has been installed to permit work to start on neutrino analysis of the data. Preliminary analyses suggest that backgrounds for contained events may be unacceptably high for atmospheric neutrino analysis without a veto shield for downgoing muons. We propose to construct a veto shield around the far detector using either MINOS scintillator system components and/or Soudan 2 veto shield components.

1 Introduction

One of the reasons for location of the MINOS far detector in the Soudan Underground Laboratory was to allow unique measurements on atmospheric neutrinos [1, 2]. MINOS is the first large underground detector which has a magnetic field. This permits measurement of muon momentum and charge which extends measurement capabilities from any existing or previous detectors. In particular, it will be possible to make significant measurements on whether atmospheric anti-neutrinos oscillate in the same way as neutrinos. Of additional importance is that the data collection and analysis on this subject can begin almost immediately, providing analysis opportunities for young colleagues and students.

The MINOS far detector installation is nearly 50% complete. The installation is proceeding very well and by July the first supermodule will be complete and the magnetic field in that section will be energized. Recently, enough data has been collected in the far detector to permit us to start to do neutrino analyses. A milestone event was the observation of the first atmospheric neutrino-induced upgoing muon. Figure 1 shows an event display for this event, including the upgoing "time track" which shows that scintillator hits higher in the detector have occurred at a later time, the signature of an upgoing muon. In May, we observed the first event which appears to have resulted from a neutrino interaction inside the detector. Figure 2 shows the event display for this event. The muon track originates inside the detector and then the muon exits through the top

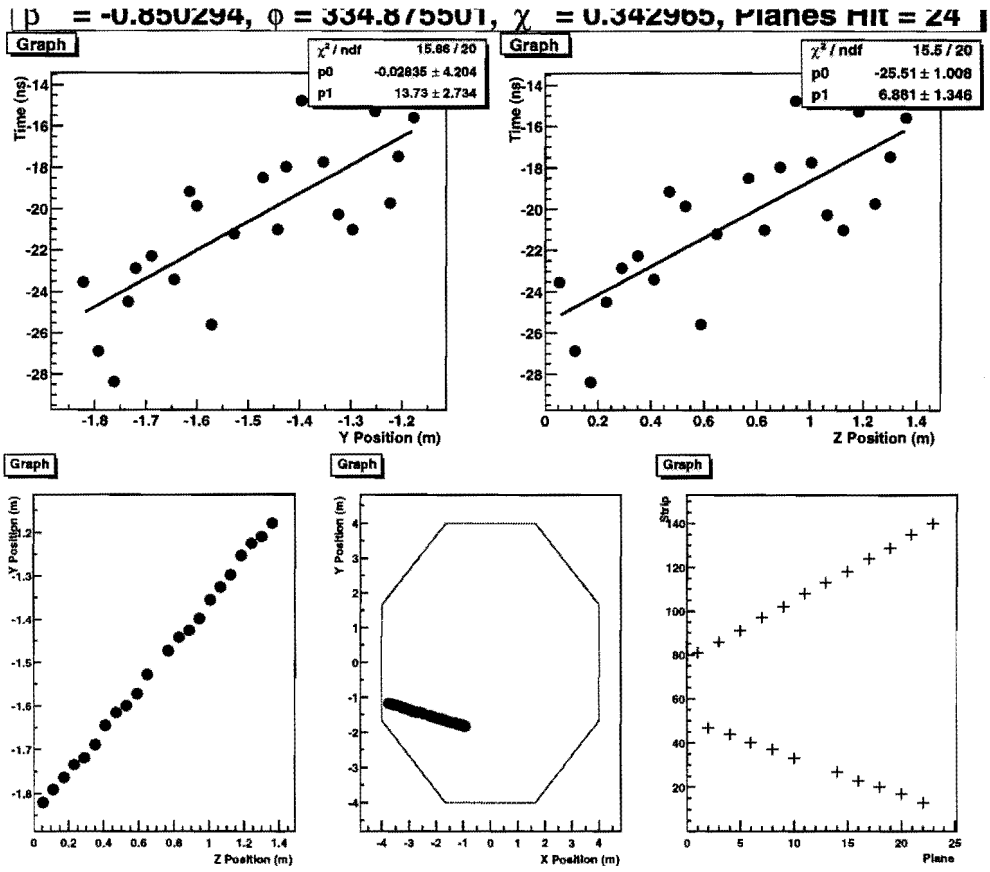

Figure 1: Event display for the first upgoing muon observed in MINOS. The several displays show the space and time tracks in the several different combinations of the detector views. The key view for determining whether the muon is travelling up or down is the time vs y, since y is the vertical direction (positive is up) in the MINOS coordinate system.

of the detector. Because the magnetic field is not yet on, the momentum of these muons was not measured. Also it should be noted that the rate at which we require these events has thus far been very small compared to our expectations come July since the detector has been turned on for data acquisition only a small fraction of the time as we install all of the electronic and safety systems.

These two events serve as a good introduction to the two basic classes of atmospheric ν_μ CC neutrino events in MINOS:

- Contained-vertex events: In these events the neutrino interacts in the detector. The interaction products, except for the muon in some cases, are contained in the detector. Neutrino events with exiting muons can be analyzed because muon momenta will be measured by track curvature. For these events, the full neutrino energy and direction are reconstructed so that an L/E analysis is possible. This makes these events the most important for precision oscillation mea-

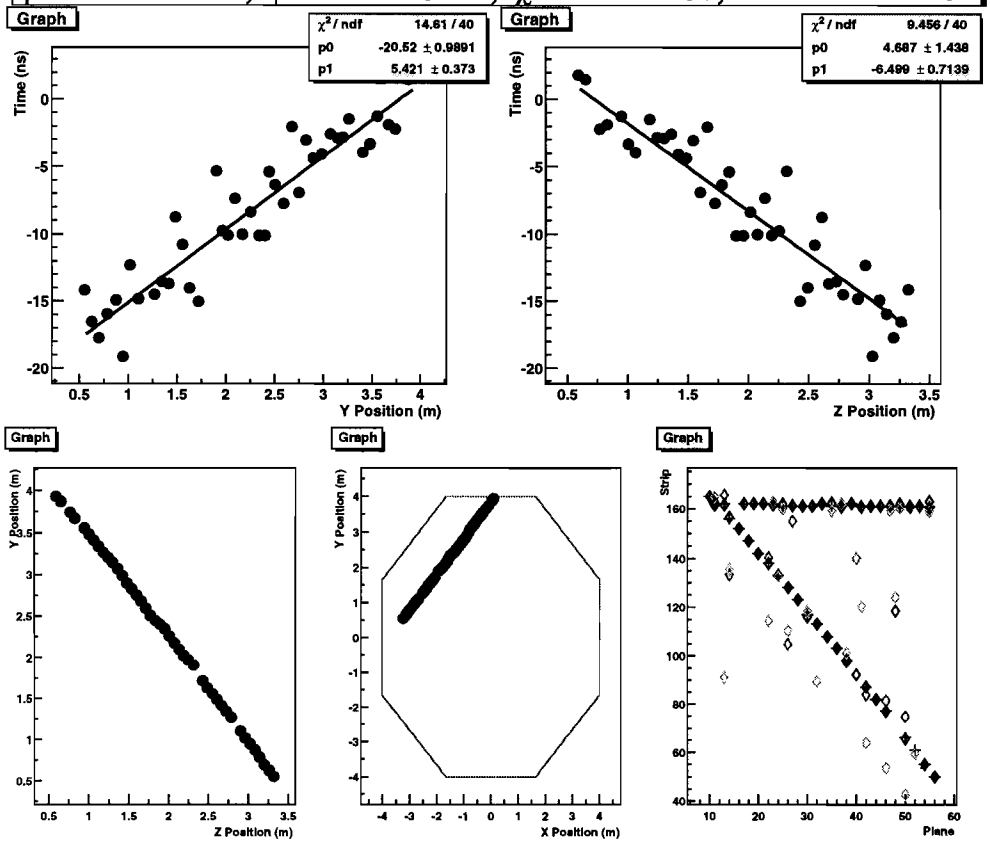

Figure 2: Event display for the second upgoing muon observed in MINOS. The several displays show the space and time tracks in the several different combinations of the detector views. The key view for determining whether the muon is travelling up or down is the time vs y, since y is the vertical direction (positive is up) in the MINOS coordinate system. This event likely originated inside the detector but our analysis systems for determining this precisely are still under development.

surements. These events are most typically generated by neutrinos with energy less than 10 GeV.

- Upgoing muons: These are muons produced in ν_μ CC interactions in the rock around and below MINOS. They are identified as resulting from neutrino interactions by time-of-flight measurement within the detector. Because the magnetic field in MINOS will permit momentum measurement for most of these muons, there is no need to distinguish between "stopping" and "throughgoing" muons as previous experiments have done. Rather, in MINOS any upgoing muon with incident energy at the detector of greater than 1 GeV will be identified as upgoing and have its momentum measured. For these events, the direction of the neutrino is reasonably well known from the direction of the muon but the muon energy only roughly corre-

lates with the initial neutrino energy [3]. Analyses taking account of both zenith angle distribution and muon energy are possible but the sensitivity to oscillations is reduced compared to the events where a complete neutrino energy reconstruction is possible. The events are induced by a very broad spectrum of neutrino energies from a few GeV to hundreds of GeV.

In addition to studies on upgoing muons, we have recently started analyses to identify contained events. Unfortunately, those first analyses have identified apparently contained events at a rate which is several times higher than could result from the interaction of atmospheric neutrinos. In order to make precise measurements, we must limit the background to no more than about 10% of the signal and furthermore be able to characterize the remaining backgrounds. The current analyses will certainly improve with time and more work. However, we believe that these initial analyses already demonstrate that a veto shield will be necessary to reduce backgrounds to the acceptable level.

The observation of the first two neutrino events accentuates the fact that the MINOS detector will be ready for making measurements on atmospheric neutrinos as soon as the magnetic field in the first Supermodule is energized early in July. However, without a shield, those analyses will be severely hampered. Hence, we are seeking a path to install a veto shield as soon as possible. It is only now that we can clearly study this issue and responsibly propose a specific shield solution. One very attractive option is to build it with MINOS scintillator system components. However, this presents another urgent timescale for making a decision which is the fact that production of scintillator system components will start to ramp-down in August of this year (and production of fiber by July).

By this proposal, we request approval for construction of a veto shield which will reduce the cosmic-ray backgrounds to the contained vertex events to an acceptable level. We cover the following topics:

1. The physics case for measurement of ν vs $\overline{\nu}$.
2. Estimated sensitivity of MINOS using atmospheric neutrinos with a veto shield.
3. Comparison with measurements from existing experiments.
4. The evidence from existing data that a shield will be necessary.
5. Set basic design requirements for the veto shield.
6. Describe two specific shield implementation options using "immediately" available components.
7. Provide cost estimates for components and installation. The total cost for construction of the shield is estimated to be \$740k.

We emphasize that several issues argue for a very rapid consideration of this proposal:

1. The window of opportunity for taking advantage of our current production for MINOS scintillator components will remain open only for a very short time. We believe this is the best means of building the shield.

2. The first half of the MINOS detector will be ready in July for start of data acquisition for atmospheric neutrino analyses. Interesting physics is there to be done immediately... with a veto shield.
3. Having a well-defined and motivated physics analysis to drive commissioning of the far detector will help deliver a completely understood detector with considerable capability for neutrino analysis already in place when the beam comes on in 2005.
4. The unfortunate delays in the planned turn-on time for the beam has created many difficult situations for students and postdocs working on MINOS. Assuring that we can engage now in world-class physics measurements will have an enormous positive impact for our young physicists.
5. The cost for building the shield is small. The timescale to build and install it is small. With immediate approval to proceed, we believe that the first Supermodule shield can be fully implemented by the end of September.

With the above considerations in mind, we request that the PAC act this June on our request for approval so that the Director can consider this summer whether this proposal is consistent with Laboratory goals, resources and NuMI Project execution... and hopefully decide to proceed with this construction as rapidly as possible.

2 Atmospheric neutrino physics with MINOS

Table 1 shows the number of neutrino and anti-neutrino events that we expect to reconstruct in MINOS in 5 years of running (which starting now is consistent with the completion of the initial beam exposure). The table shows the numbers for no oscillations and with oscillations with "nominal" oscillation parameters $\Delta m^2 = 0.003$ eV^2 and $\sin^2 2\theta = 1.0$. A 50 cm fiducial cut inside the outer surface of the detector is required

	ν_μ $\Delta m^2 = 0$	$\overline{\nu_\mu}$ $\Delta m^2 = 0$	ν_μ $\Delta m^2 = 0.003$ eV^2	$\overline{\nu_\mu}$ $\Delta m^2 = 0.003$ eV^2
Reconstructed Contained Vertex Events	620	400	440	260
Upgoing through-going and stopping muons	400	160	280	120

Table 1: Number of reconstructed atmospheric ν_μ and $\overline{\nu_\mu}$ events expected in five years of running with MINOS. The numbers are shown for contained vertex events and upgoing through-going and stopping muons and for no oscillations and the "nominal" oscillation expection with $\Delta m^2 = 0.003$ eV^2 and $\sin^2 2\theta = 1.0$.

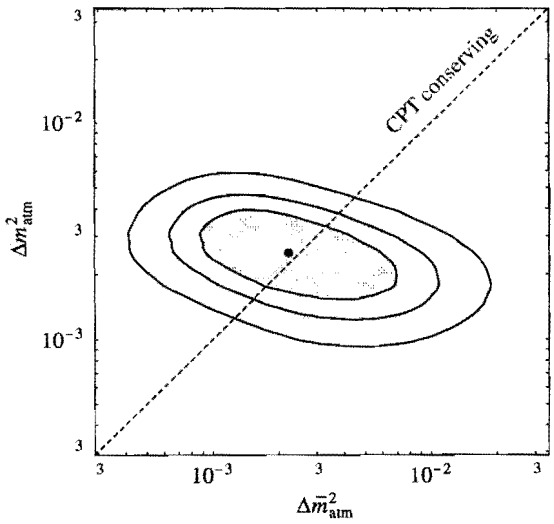

Figure 3: Allowed regions for Δm^2 for ν_μ and for $\overline{\nu_\mu}$ as calculated by Strumia in a fit to data from Super-Kamiokande [8] The contours show the 68%, 90% and 99% CL regions.

for the vertex position of contained-vertex events so that the mass-years exposure in this time is 24 kT years.

Figure 4 shows the reconstruction efficiency for atmospheric CC ν_μ and $\overline{\nu_\mu}$ events in MINOS vs the muon momentum in the event. Figure 5 shows the efficiencies vs the true neutrino energy for CC ν_μ and $\overline{\nu_\mu}$. In both figures the saturation in efficiency at about 70% at relatively high energies is primarily due to the planar geometry of the detector for events incident nearly parallel to the planes. We use reconstructed quantities for the results presented here. If a muon track is reconstructed, the probability is >98% that the charge has been determined correctly. Likewise, if a track has been reconstructed the probability is also >98% that the direction has been correctly determined by timing and event topology.

2.1 Comparison of ν_μ and $\overline{\nu_\mu}$ oscillations

The magnetic field of MINOS will enable several unique measurements compared to previous atmospheric neutrino experiments. We think that the most compelling and important measurement will be a comparison of oscillations between ν_μ and $\overline{\nu_\mu}$. This is accomplished by measuring the curvature of muons in the magnetic field of MINOS. We will be able to identify the charge, and hence whether the muon was produced by a neutrino or anti-neutrino. No previous measurements exist which differentiate between the two.

Differences in the disappearance rate of neutrinos and anti-neutrinos requires CPT violation. There have been several theoretical papers in the last year which have suggested that this may be the case [5, 4, 6, 7, 8]. Nobody knows what levels of CPT violation are possible from a theoretical basis. However, it is generally understood that non-local theories, such as string theories, may exhibit CPT violation. Figure 3 shows the possible range of Δm^2 for $\overline{\nu_\mu}$ vs ν_μ based on a fit to data from Super-Kamiokande.

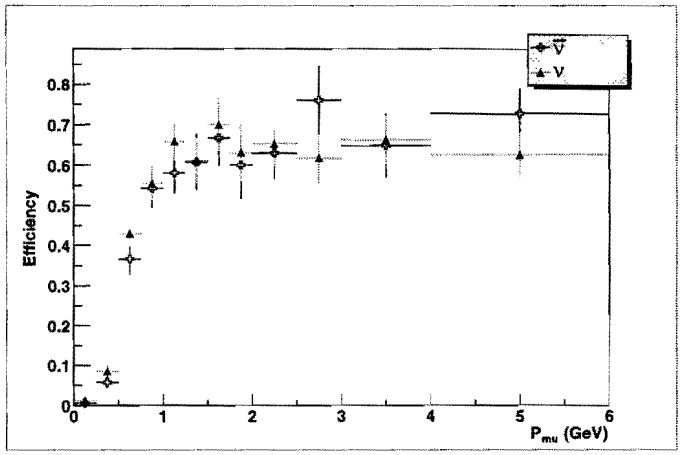

Figure 4: Reconstruction efficiency for CC events vs muon momentum. The efficiencies are identical between ν_μ and $\overline{\nu_\mu}$ events for a given muon momentum. The plateau in efficiency is due to events incident nearly parallel to the plates of the detector. Essentially all events with a reconstructed muon also have the direction and charge determined correctly.

The Super-Kamiokande collaboration has just presented somewhat more stringent constraints based on updated analyses just presented at Neutrino 2002, but qualitatively the allowed region of Δm^2 for $\overline{\nu_\mu}$ is similar to shown here and still much larger than for ν_μ [9].

In MINOS, we anticipate making several measurements which will provide sensitivity to whether ν_μ and $\overline{\nu_\mu}$ oscillate in the same way:

- Angular and energy distributions of all events.
- L/E distributions for all contained-vertex events.
- Up/Down ratio vs angle and energy for all contained vertex events.

The distributions for ν_μ and $\overline{\nu_\mu}$ will be compared and an overall likelihood function will be calculated which determines whether the two oscillate in the same way. The information in these distributions is correlated but the relative systematic uncertainties are different for each distribution. The Up/Down ratio has the disadvantage that it divides the statistical power of the data but has the distinct advantage that the systematic uncertainty is essentially zero. We have not yet had time to develop the relatively sophisticated Monte Carlo tools which are essential to properly calculate the sensitivities using these correlated functions. Here we present some simpler, but ultimately less sensitive calculations which provide first estimates of the sensitivity that we expect to differences in oscillations.

We note that the systematic uncertainties on the ratio between ν_μ and $\overline{\nu_\mu}$ will be much smaller than on the calculation of the absolute oscillations for either. This is because the systematic uncertainties on atmospheric neutrino fluxes almost completely cancel in taking ratios between the two

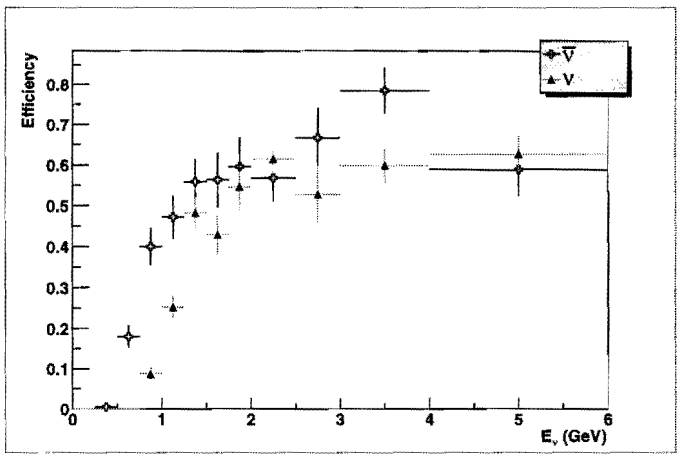

Figure 5: Reconstruction efficiency for CC ν_μ and $\overline{\nu_\mu}$ events vs neutrino energy. The plateau in efficiency is primarily due to events incident nearly parallel to the plates of the detector but there is also some contribution from high y events at higher neutrino energies. Essentially all events with a reconstructed muon also have the direction and charge determined correctly.

types of events. The systematic uncertainty on the flux of upgoing muons will remain somewhat higher than for the contained-vertex events. This is due to the relative importance of the y-distribution in these events since the muon must travel a long distance to reach the detector and for equal energy the effective target for anti-neutrinos will be larger than for neutrinos.

Hence, the contained-vertex events are of great importance to making a precision measurement of the difference in oscillations between ν_μ and $\overline{\nu_\mu}$. We believe that limiting the background from these events to a level no greater than 10% of the number of contained neutrino-induced events is well justified. We also wish to be able to sufficiently characterize the likely remaining background so that the remaining systematic uncertainty due to this will be no more than 2% once all corrections are applied.

Table 2 presents a summary of the systematic uncertainties for comparison of ν_μ and $\overline{\nu_\mu}$ measurements. Although these estimates are preliminary, they provide a sufficient basis to evaluate the physics potential of installing a shield around MINOS. We provide estimates based both on current data and on possible improvements which may result from new data in the next few years. These data include precision measurements from MINOS on neutrino oscillation parameters, new hadron production measurements from HARP and E907, new atmospheric neutrino flux calculations using full 3-dimensional approaches combined with the new hadron production data and perhaps new information on the relative cross sections using data from the MINOS near detector.

In this document, we present only the start of what will become the

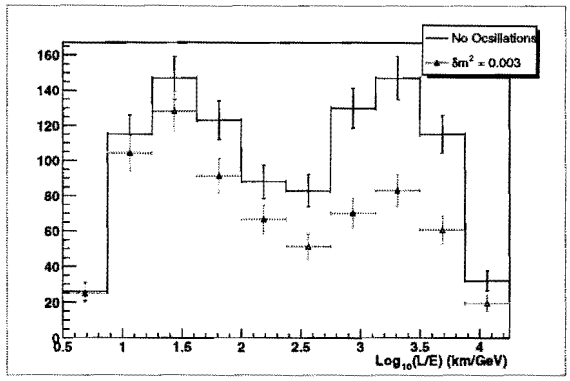

Figure 6: The reconstructed L/E (km/GeV) expected for ν_μ with no oscillations and with the nominal oscillation parameters of $\Delta m^2 = 0.003$ eV^2 and $\sin^2 2\theta = 1.0$.

Source of Uncertainty	% Now	Expected % in 2007
Atmospheric +/- hadron ratio	3	1
K/pi ratio	3	1
Cross Sections	5	3?
Reconstruction Efficiency (due to y dist.)	5	3
Total for contained events	8	5
Upgoing muon effective target	10	10
Total for upgoing muons	13	12

Table 2: Estimates of systematic uncertainties in comparison of ν_μ and $\overline{\nu_\mu}$ measurements and from various sources. Estimates are provided based on currently available data and based on new data which are likely to become available during the running period to collect this data in MINOS.

ultimate analysis for atmospheric neutrinos in MINOS. The main result which we present here is based on the L/E distribution calculated for the atmospheric neutrinos and antineutrinos. The event reconstruction efficiencies have already been presented. Figure 6 shows the L/E distribution expected for the neutrinos with no oscillations and with the nominal oscillation parameters. Figure 7 shows the ratio of L/E for the neutrinos with and without oscillations. The error bars show the statistical uncertainties. Figure 8 shows the L/E ratio between neutrinos and anti-neutrinos. The statistical error bars are the convolution of those for the neutrinos and anti-neutrinos. The systematic errors on this double ratio are correlated between the bins and are as presented in table 2. Figure 9 shows the χ^2 between the neutrino and anti-neutrino distributions assuming the nominal atmospheric parameters for the neutrinos and a variety of Δm^2 for the anti-neutrinos. Finally, figure 10 shows the probability of χ^2 for the same situation.

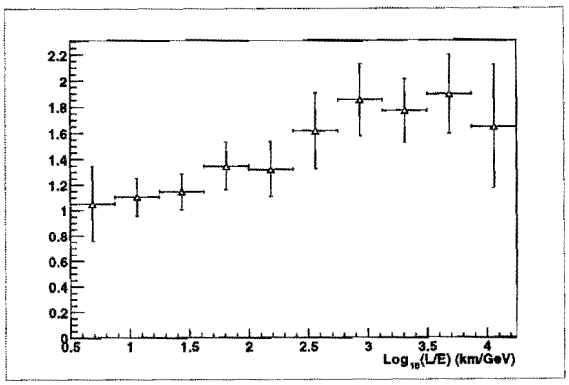

Figure 7: The ratio of reconstructed L/E (km/GeV) expected for ν_μ with no oscillations and with the nominal oscillation parameters of $\Delta m^2 = 0.003$ eV^2 and $\sin^2 2\theta = 1.0$.

The same set of plots can be made except where we take account of the fact that oscillation parameters for ν_μ will be relatively well measured by MINOS from beam running during the integration period for the atmospheric neutrino exposure. In this case, we can use the total statistics of the atmospheric ν_μ events to cancel all of the dominant systematic uncertainties and directly calculate the expected L/E distribution for those neutrinos based on the integrated number of events. A relatively small additional systematic uncertainty of about 5% will apply which is added in quadrature with the remaining systematic uncertainty on the normalization. Figure 11 shows the probability of χ^2 under this assumption. We note that our precision measurement of oscillation parameters with the beam in MINOS will simultaneously improve our measurement of the anti-neutrino oscillation parameters from the atmospheric neutrino data! (Note that the rate of anti-neutrino events in the neutrino beam is too small to contribute directly to a measurement of oscillation parameters while running in neutrino mode.

Figure 12 shows the ratio of the number of events vs cos(zenith) for upgoing positive muons compared to upgoing negative muons assuming nominal oscillation parameters for neutrinos and a variety of Δm^2 for the anti-neutrinos as shown. The χ^2/DOF vs Δm^2 is shown in table 3, assuming systematic uncertainties as presented in table 2. Note that this analysis does not yet take account of the energy of the muons (lack of time). We combine this χ^2 in an overall probability with the contained vertex events.

Figure 13 shows the combined probability as a function of Δm^2 for $\overline{\nu_\mu}$ assuming fixed oscillation parameters for oscillation of ν_μ at the nominal values which have been measured by MINOS by 2007. We note that the precision of the combined measurement is dominated by the contained-vertex events.

Although we have not yet performed any detailed calculation, we note

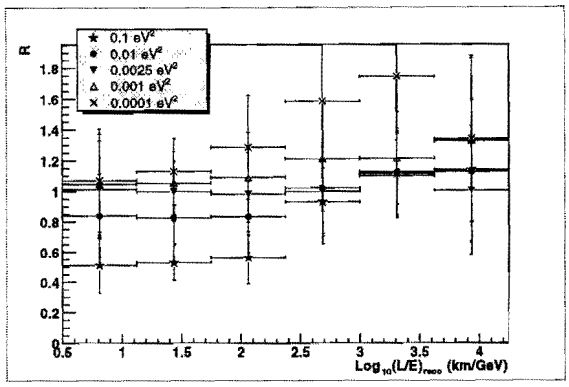

Figure 8: The reconstructed L/E (km/GeV) ratio for ν_μ and $\overline{\nu_\mu}$ vs Δm^2 for $\overline{\nu_\mu}$ given ν_μ with the nominal oscillation parameters of $\Delta m^2 = 0.003$ eV^2 and $\sin^2 2\theta = 1.0$. The statistical error bars include the statistical fluctuations on both the ν_μ and $\overline{\nu_\mu}$.

that our measurements will also provide sensitivity to difference in the mixing strength. The up/down ratio comparison between ν_μ and $\overline{\nu_\mu}$ should provide the best measurement of the relative total oscillation probability, and therefor the mixing angle, for the two types of events. In five years of running, this measurement will clearly be dominated by statistical uncertainty. Based on our expected statistics in this time, we will be able to detect a difference of 16% in the oscillation probability (at one σ).

$\overline{\nu_\mu}$ Δm^2 (eV^2)	χ^2/DOF
0.0001	4.0
0.001	1.9
0.003	1.0
0.005	1.5
0.008	2.1
0.01	2.7

Table 3: The χ^2/DOF calculated between the zenith distribution of upgoing positive and negative muons for different values of $\overline{\nu_\mu}$ and for $\Delta m^2 = 0.003$ eV^2 for ν_μ.

2.2 Other Unique Neutrino Measurements in MINOS

Other measurements which can be done because of the magnetic field include

- Again using the magnetic field, we will provide complete neutrino

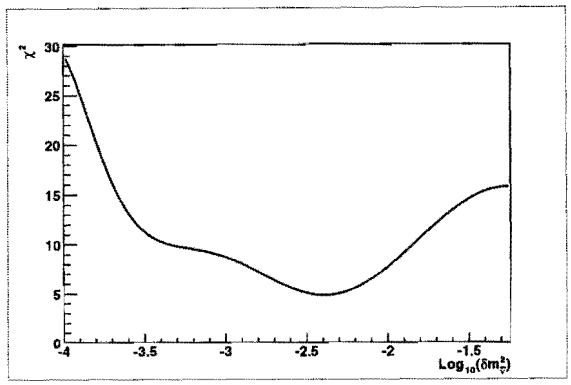

Figure 9: The χ^2 between the reconstructed L/E (km/GeV) ratio for ν_μ and $\overline{\nu_\mu}$ expected for ν_μ with the nominal oscillation parameters of $\Delta m^2 = 0.003$ eV^2 and $\sin^2 2\theta = 1.0$. The statistical errors used include the fluctuations on both the ν_μ and $\overline{\nu_\mu}$.

energy measurements up to relatively high energies for the contained-vertex interactions. Combined with the contained events this will provide a relatively good high energy L/E measurement compared to existing detectors.

- We will measure the muon momentum for most of the upgoing muons which may provide additional constraints on oscillation parameters compared to existing measurements and provide a high-energy sample of events (the muons will look straight) which accentuates sensitivity to astrophysical point sources of neutrinos. (MINOS can measure curvature in muons up to momenta $\approx$ 70 GeV/c.)
- We will use calorimetric response to search for very high energy muons (10 TeV and above). Even a single event of this type which points towards a known astrophysical accelerator may be very interesting. Because MINOS is a much better EM calorimeter than previous detectors we can offer new constraints on this type of event (and perhaps even different constraints than detectors like Amanda?)

We do not further develop the description of these physics measurement possibilities in this proposal since they do not depend closely on the installation of the shield.

3 The need for a shield for contained-vertex events

The rate of downgoing muons entering MINOS is about 10^5 times higher than the rate of neutrino interactions in MINOS. Backgrounds to contained neutrino interactions may be generated when a downgoing muon

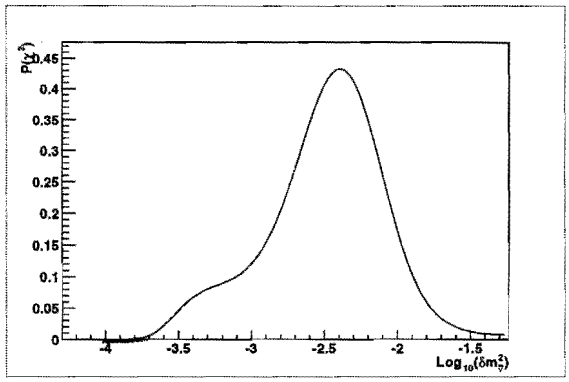

Figure 10: The probability of χ^2 between the reconstructed L/E (km/GeV) ratio for ν_μ and $\overline{\nu_\mu}$ expected for ν_μ with the nominal oscillation parameters of $\Delta m^2 = 0.003$ eV^2 and $\sin^2 2\theta = 1.0$. The statistical errors used include the fluctuations on both the ν_μ and $\overline{\nu_\mu}$.

(typical energy around 200 GeV) enters the detector through a gap between scintillator planes (moving near to parallel with the detector planes) and then interacts in a plane of steel to produce an apparent contained event. The interacting muon may or may not be finally observed but if it is observed only following the interaction it could just as well have resulted from a neutrino interaction. Hence, in order to properly veto such background events it is important to observe the muon before it enters the detector, on its way down. An additional class of problematic events are low energy downgoing muons which again enter the detector through a gap and then scatter in the steel and thus appear to originate from a neutrino interaction inside of the detector. These can exactly mimic low-energy CC ν_μ interactions.

At this time, we have two pieces of evidence that a shield will be necessary for analysis of contained and contained vertex events.

1. Our attempts to date at identifying contained events has yielded many more events than are possible from neutrino interactions. We observed roughly 200 times more showering events and 30 times more track-like events than expected from neutrino interactions with observed energies in the detector greater than 1 GeV. Further inspection by eye of event displays for the track-like events lead us to believe that most of that background results from current commissioning issues in both hardware and software. This will likely be improved in the future, but probably not to the necessary level unless a shield is built.

   Figure 14 shows the reconstructed vertex positions of events (actual data, not Monte Carlo!) where a muon-like track has ended inside of the detector. Most of the events are clearly downgoing, low-momentum muons which enter the detector and come to a stop.

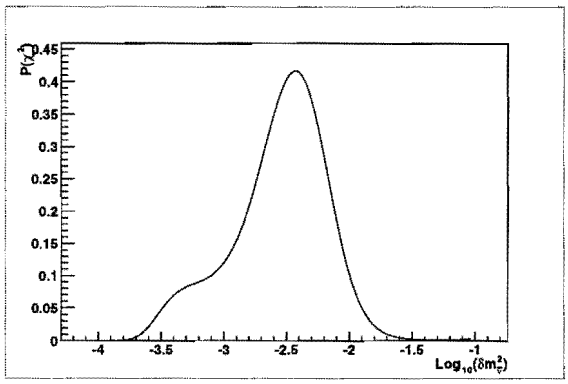

Figure 11: The probability of χ^2 between the reconstructed L/E (km/GeV) ratio for ν_μ and $\overline{\nu_\mu}$ expected for ν_μ with the nominal oscillation parameters of $\Delta m^2 = 0.003$ eV^2 and $\sin^2 2\theta = 1.0$. The statistical error bars include only the statistical fluctuations on the $\overline{\nu_\mu}$ events but an additional 5% systematic error has been included in the relative normalization.

Their "vertices" are clearly and properly reconstructed right at the top edges of the detector. However, a number of events have vertices which reconstruct well inside our planned fiducial volume defined by a radius of 3.5 m. Close inspection of displays for these events shows that they are really all downgoing muons where either a hardware problem resulted in some missing hits and/or a reconstruction/demultiplexing problem.

We estimate that a background of 10% is acceptable for our analyses (correctable down to 2% by adequate characterization of the backgrounds). Hence we require that a shield provide reduction in the background by a factor of 20-50.

2. The Soudan 2 detector required a veto shield with about a factor of 80 reduction. However, Soudan 2 also had relatively fewer cracks than MINOS (which viewed side-on is mostly cracks!). Offsetting the fact that MINOS has more cracks is the fact that we will only attempt to look at events which are relatively high energy compared to those observed in Soudan 2 and the average density is higher. An important class of background events in Soudan 2 were showers with energy less than 500 MeV which are not relevant in MINOS. However, Soudan 2 also observed relatively higher energy track-like events which needed to be vetoed with their shield.

4 Design requirements for a shield

We have set the following design requirements for a shield, based on our preliminary contained event analysis:

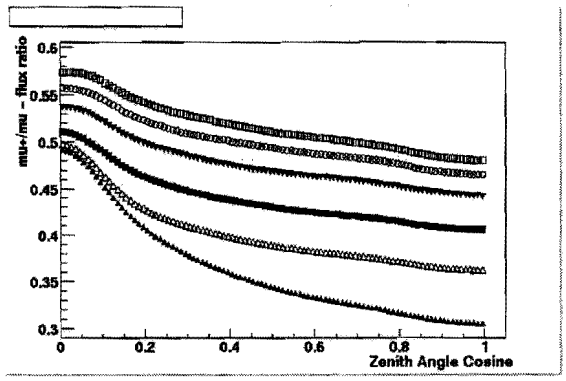

Figure 12: The ratio of the number of events at each cos(zenith) for upgoing positive and negative muons for ν_μ with the nominal oscillation parameters of $\Delta m^2 = 0.003$ eV^2 and $\sin^2 2\theta = 1.0$ and for different values of Δm^2 for $\overline{\nu_\mu}$ for each curve on the plot. The values of Δm^2 for $\overline{\nu_\mu}$ are 0.0001, 0.001, 0.003, 0.005, 0.008 and 0.01 eV^2 running from the top to the bottom curve.

1. All downgoing muons which pass through the detector should pass through at least one layer of shield first.
2. The shield design should incorporate two layers of detector on the top in order to get very high efficiency. The efficiency should be >98%.
3. Fast-timing is attractive as it may be useful for helping to keep the fiducial volume of the detector as large as possible by providing an additional discriminant for containment based on time.
4. Some localization of readout should be provided to assist in characterizing backgrounds. A 30-40 cm wide readout running transverse to the detector planes is acceptable.
5. Rapid deployment should be possible. This means keeping engineering and development very simple and using existing components as much as possible.
6. Costs need to be kept very low. A mono-layer shield has equivalent area as 13 MINOS detector planes. Although this is only 2.7% of the MINOS far detector that is comparable to the entire area of scintillator in most big collider scintillator-based hadron calorimeters.

5 Technology options

We think there are only two technology options which can meet the design criteria described above: MINOS scintillator system components and/or re-use of Soudan 2 shield components. We comment briefly on some of the relevant issues which have been used in the evaluation:

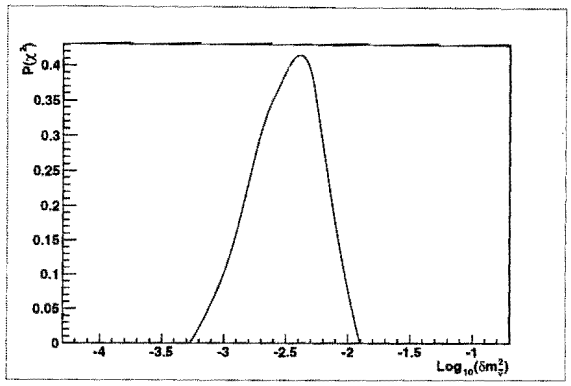

Figure 13: The combined probability of χ^2 for both contained vertex events and upgoing muons for ν_μ with the nominal oscillation parameters of $\Delta m^2 = 0.003$ eV^2 and $\sin^2 2\theta = 1.0$ and various Δm^2 as shown on the abscissa for $\overline{\nu_\mu}$. The statistical errors used include only the statistical fluctuations on the $\overline{\nu_\mu}$ events but an additional 5% systematic error has been included in the relative normalization.

- MINOS scintillator components
  1. Fast timing: The MINOS scintillator shield provides a time resolution of about 2.6 ns per layer for a muon crossing.
  2. Cost: We know the production cost for MINOS scintillator components very well and incremental cost of production of these components presents excellent value given the investment which already exists for production of MINOS planes. However, the ability to produce at good costs lasts only a few more months before current purchase contracts are completed and before we begin to ramp-down production. We already know that MINOS scintillator planes provide excellent value for large area coverage, regardless of technology.
  3. Use of MINOS scintillator components "as is" avoids the time and expense of any significant engineering design for detector components. The modules themselves are mechanically very strong and light and require only a modest support frame.
  4. Use of MINOS scintillator modules permits us to completely integrate the entire readout system with the existing detector trivially. We continue to have only one technology to maintain so once it is built the ongoing costs compared to the existing detector are negligible.
- Soudan 2 shield components
  1. The Soudan 2 shield consists of aluminum proportional tubes. These have been used reliably for many years. For use in MINOS, they would need to be dismounted from their current location. It will be necessary to build some new electronics for

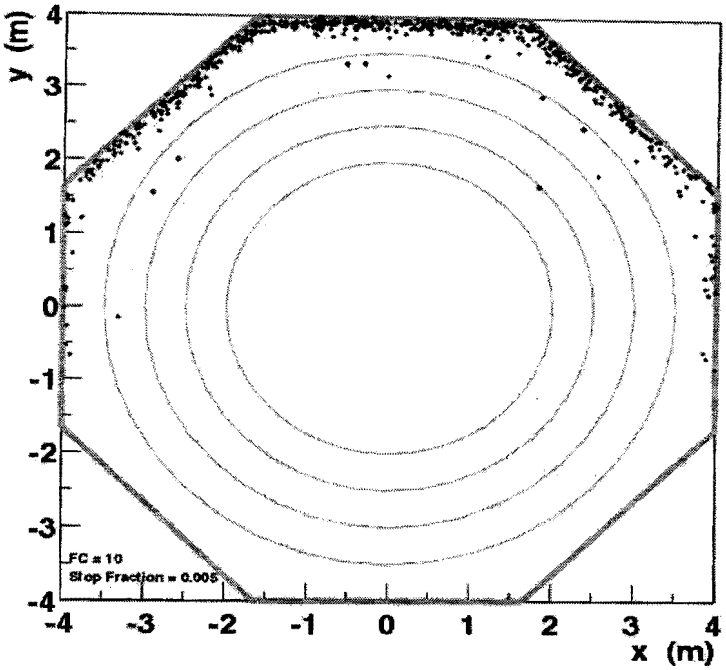

Figure 14: Reconstructed vertex positions of events (actual data, not Monte Carlo!) where a muon-like track has ended inside of the detector. Most of the events are clearly downgoing, low-momentum muons which enter the detector and come to a stop. Their "vertices" are clearly and properly reconstructed right at the top edges of the detector. However, a number of events have vertices which reconstruct well inside our planned fiducial volume defined by a radius of 3.5 m.

extended use in MINOS. Finally, the existing gas system will require refurbishment for use in MINOS. The cost for these items are the the effective "production costs" for this system.

2. The efficiency of this system as a veto shield is already well understood from Soudan 2 experience.
3. The support structure requirements for these tubes is somewhat more due to their higher weight but does not significantly add to the cost.
4. We would need to maintain a gas system throughout MINOS running.
5. The relative efficiency per plane is less. However, the tubes come in pairs of offset hexagonal planes delivering overall high efficiency.

A final possibility is to use a hybrid approach where a layer of MINOS scintillator provides fast timing but a layer of Soudan 2 tubes provide

additional veto efficiency.

6 A reference shield design

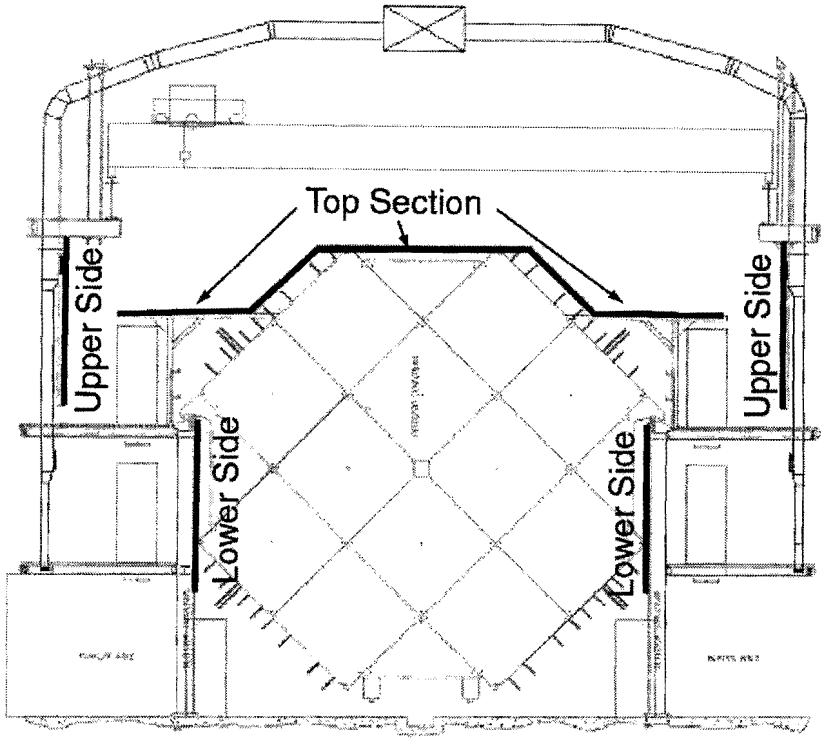

Figure 15: The locations of shield components around the MINOS detector. The shield consists of a top section, upper side sections and lower side sections. The top section consists of a central part, and wings on each side of the detector. The top shield is designed to continue to permit use of the access bridge to the top of the detector and shield.

We have chosen MINOS scintillator modules for the reference design for the MINOS veto shield for the following reasons:

1. Fast timing will maximize the fiducial volume: Events near the edge may have relatively short muon tracks for which the maximum lever arm for track reconstruction will add significantly to the total detector mass. Every 10 cm of detector adds 6% to the fiducial mass. We expect that the fast timing will add an effective mass at least this much.
2. The MINOS modules are the easiest and fastest thing for us to implement. They are light and easy to handle. We have the construction

process fully operational and it is almost trivial for us to make very small changes in the production rates of appropriate types of components in order to meet the shield demands. The scintillator system components are built well ahead of the installation demands and no detector construction or installation milestones will be affected.

3. Once installed, maintenance of this system will be no different than for the rest of the detector and the overall maintenance and running costs will be less than with a gas system.
4. We propose that we implement a reconfiguration of 4% of the detector planes currently planned within the project to maximize the total physics output of MINOS. Under this plan, new funds are required only for the construction of the support system and installation of the modules. The cost for this is \$100k compared to \$300k of spending not currently planned within the existing project for construction with the proportional tubes. A partial modification to this plan is to plan for additional construction for half of the shield as a ramp-down activity in our scintillator production facilities.
5. Should it be necessary, the non-module components of the shield can be called to duty in the main detector as spares. Additionally, we will need to over-build some small quantity of modules ($\approx$0.5%) to assure that we have enough good modules on hand for completion of the detector.
6. We believe that this approach will have the smallest impact on the existing project and in several ways benefits the existing project.

Here, we present our reference design for the veto shield based on MINOS scintillator components. The reference design consists of the following:

1. The Top Shield: The top of the detector will be covered with two layers of MINOS scintillator modules. The modules will be supported on an iron-tube structure which will be supported in turn by the support structure for the MINOS planes and in part by the planes themselves. The supports will be installed transverse to the axis of the hall and above the top of the detector. The top layer will be shaped so that the existing access bridge which runs on rails over the top of the detector may continue to be used. It will be used for installation of the shield. Figure 15 shows a drawing of the detector with the proposed locations for shield components. The scintillator modules will run parallel to the axis of the detector hall. A total length of two 8 meter modules is required to cover the length of each half of the detector. We will study whether one or two layers is necessary in this location. A single layer requires the equivalent of 6 planes of scintillator detector components or 1.2% of the far detector. Hence, a double layer is equivalent to 12 planes or 2.4%.
2. The Upper Side Shield: The shields on the sides of the detector are split into an upper section and a lower section. This is necessary due to the support structure and walkways along the sides of the detectors. The solid angle coverage, fractional detector coverage

Item	Number required	Fraction of Fardet	Comments
Scintillator Modules	184	4.5	
Clear Fiber Cables	368	4.8%	Appropriate lengths for module locations
Hamamatsu M16 PMTs	66	4.5%	
PMT Boxes	28	5.8%	Special built boxes. Some cost off project
Front-end electronics	28	5.8%	boards and cables. Use some spares
Readout electronics	18	5%	VARC boards. Use some spares. No new crates

Table 4: Scintillator system components needed for the shield.

and associated muon flux are smaller for the side shields than for the top shield. Hence, the side shields will be only a single layer (subject to confirmation that this is adequate). Like the top shield, the length of 2 8 m scintillator modules will provide coverage for each supermodule. The upper side shield is located near the cavern walls above the upper catwalk. This is equivalent to 6.5 planes or 1.3% of the far detector.

3. The Lower Side Shield: The lower side shields are located between the detector and the support structure below the support ears of the steel. Like the upper shield, it is a single layer two module in length and 4 modules high for each side for each supermodule. This is equivalent to 6.5 planes or 1.3% of the far detector.

Fibers are routed to PMT boxes where the fibers from eight adjacent strips are summed onto each PMT pixel. Fibers from multiple shield layers will be routed to separate PMTs and electronics front-ends in order to avoid any correlated inefficiencies due to single photo-electrons in the detector. One possiblility is to run the electronics at a threshold above a single photo-electron in order to remove all of this type of inefficiency. We will make use of standard scintillator modules, mostly-standard clear fiber cables (some will be a bit longer than normal detector cables), standard PMTs and electronics and PMT boxes which have a different internal light routing pattern. Only the PMT boxes really differ significantly from other detector components. There is room in each of the PMT racks where PMT boxes are currently located for additional boxes. Other than front-end electronics channels, no additional readout electronics or DAQ electronics is needed.

Table 4 lists the scintillator system components needed for the full shield implementation.

The support structure on the top of the detector consists of a total of 20 tubular steel structures with appropriate cross-bracing as shown in reference [12], "Prototype Veto Shield Construction". The structures are supported by the top ears of steel planes in the detector and by vertical supports which hold it above the support structure at the sides of the detector. The support structures run transverse to the axis of the detector hall at a pitch of 2m. The modules simply sit directly on the support structure supported directly by the steel tubes every 2m. They

Item	Cost ($k)	Comments
Scintillator Modules	368	Includes scintillator and WLS fiber
Readout Components	272	Clear fiber cables, PMTs, electronics
Support structure and installation	100	(includes 50% contingency)
Total	740	

Table 5: Costs for the reference design shield. Only the costs for the support structure and installation are not currently within the existing project assuming that we are allowed to reconfigure some of the components to maximize physics output.

are clamped at the ends and middle to keep them from moving.

The support structure on the sides of the detector consist of vertical steel channels which are located every 2 m along the length of the modules. The modules will be bolted to the channels using brackets which hold the module at the top and the bottom at each vertical support location.

7 Cost for the reference design

Based on actual production costs, we have estimated the full cost of the reference veto shield. These are shown in table 5. The cost for components is about 1/2 for scintillator modules and 1/2 for all of the readout components (clear fiber cables, PMTs, PMT boxes, electronics). The costs presented here include all overheads and are estimated based on well-known production costs. These costs do not include any explicit contingency but do contain some "internal" contingency in the individual component estimates which is known to make these production costs adequate. The cost for the construction of the support structure and installation includes a 50% contingency.

7.1 Implementation and installation

We are already planning implementation of 1/4 of the veto shield as a prototype for the full shield. Various MINOS collaborating institutions have pooled money to pay for the installation of the prototype, a total cost of about $25k. We plan to borrow the scintillator system components (for now) from the project. We assume that this will be complete by the end of June but at this writing have not yet received permission to proceed with this installation. Should we be given approval to proceed in July, we plan to stage the implementation of the installation of the full veto shield in the following way:

1. Fabricate and install complete top support structure by August 14.
2. Install complete top layer of scintillator modules by August 30.
3. Install upper sides by September 15.
4. Install lower sides by August 30.

5. Install shield for second supermodule within 3 months following its completion.

We expect that the rate of installation of MINOS planes will not be significantly effected by installation of the shield. Specifically, we are confident that the project schedule of 6.4 planes per week on average can be maintained. All technician manpower for shield fabrication and installation will be accounted separately from project work and paid for from various university funds. All special materials required will be purchased from university funds.

The fabrication of the steel tube structure will be done by the surface crew at Soudan. The underground mechanical installation will be done by a combination of mine-crew and university technicians. The hookup and testing of the readout will be done by physicists. We will schedule installation work using any minecrew as overtime activity if there is any interference with maintaining the installation schedule for the detector.

Additional details of some of the planning for installation of the prototype shield may be found in the accompanying construction document in the appendix.

7.2 Safety issues

The main installation work will be done by the minecrew who are currently working on installation of the far detector planes. Hence, they are very familiar with the working environment at the mine and the handling of these components. Other than safety concerns which are a part of the usual operations at the mine, we have identified the following issues which have some differences with the veto shield that are worth consideration:

- The support structure: We need to make sure that the support structure has appropriate strength and rigidity. The scintillator modules are quite light, only about 200 pounds per module and the corresponding support structure is quite simple. We have had the design reviewed by two sets of mechanical engineers to assure that nothing has been missed. It has also been reviewed by the Soudan Safety committee and the Fermilab Safety Committee. We welcome any additional reviews which may be deemed necessary.
- Possible damage during installation: It is possible that some clear fiber cables in the detector, or possibly even a protruding scintillator end manifold could be damaged during installation by being struck with a piece of support structure as it is being installed. Any such damage must be quite local. Clear cables can be replaced and are the most likely thing which might be damaged. Modules are actually quite robust and we anticipate nothing worse than a light leak which would need to be repaired. However, we will exercise particular care in this activity to avoid any damage. Installation of the modules also presents some possibility of damage, but probably only to clear cables which can be replaced.
- Installation of the shield above the detector covers the central detector from overhead water sprinklers. Because all of the scintillator

is completely enclosed in aluminum casings it is our analysis that this does not present any additional fire hazard. Minnesota code officials have preliminarily concurred that this installation is acceptable. Fermilab safety officials have also reviewed the idea. However, we are again open to additional review.

- During the installation, there is a danger that a person working on the access bridge could fall. The danger is not different than if accessing the top of MINOS but the amount of time needed for such access is relatively large compared to normal work on planes. However, we do have such experience and a clear set of procedures have been implemented to ensure work in this area is done safely.

7.3 The Alternative Shield: Proportional Tubes

If for some reason it is impossible to find the means to build the shield using MINOS scintillator components, we would like to build the shield using the existing proportional tubes from the Soudan 2 veto shield. We do not describe this option in any significant detail here, but we have made a substantial study of this backup option which is fully described in a stand-alone document [13]. As already mentioned, the total cost for that shield would be less but the effective fiducial volume will also be less due to the lack of fast timing and the amount of completely "new money" that clearly needs to be generated is substantially more. However, we most definitely would prefer to have this shield than no shield at all!

The work around the MINOS detector is very similar to that for the scintillator modules. The current proportional tubes would need to be removed from their current position, refurbished and tested and then installed around MINOS. The gas system would have to be re-furbished and setup in the MINOS hall. New versions of the far detector electronics would need to be built to accomodate the smaller and different pulses from the proportional tubes. However, the basic front-end is effectively identical to the remaining MINOS electronics in most ways and it reads out into the normal MINOS data acquisition stream just as the scintillator system.

Because of the somewhat more complex setup required for this option, the implementation of the shield for the first supermodule would likely be delayed from the schedule which is possible using scintillator modules by a few months. We still expect that it could be complete by the end of this year however. We expect that the installation time for the second supermodule would be nearly identical to that for the scintillator modules.

Again, we stress that our main interest is that we get some veto shield with at least a factor of ≈ 50 rejection power on downgoing muons. We take this as the overwhelming design requirement for the shield and should funding for some reason be feasible for this option and not for the scintillator option then we are fully prepared to undertake this implementation. We invite the truly interested reader to review the thorough stand-alone document describing this implementation listed in reference [13].

8 Summary

Preliminary data show that a veto shield will be very important to analysis of contained atmospheric neutrino events in MINOS. We believe that an exciting opportunity exists to use atmospheric neutrinos and anti-neutrinos to probe the possibility of CPT violation in neutrino oscillations. The results of this study are likely to be much less definitive without a veto shield. The MINOS scintillator components present an attractive means for construction of this shield, but production is ending soon. Hence, if we wish to take this opportunity we must act quickly to decide to implement the shield. The time required to install the shield is small as is the cost. We request immediate approval to proceed with construction of this shield.

References

[1] P875: A Long-baseline Neutrino Oscillation Experiment at Fermilab, The MINOS Collaboration, February 1995.

[2] Letter from the Fermilab Director, 1995.

[3] MACRO Collaboration, "Estimate of the energy of upgoing muons with multiple Coulomb scattering", Proceedings of the NATO ARW on Cosmic Radiations: from Astronomy to Particle Physics, Oujda (Morocco), 21-23 March 2001. Also in talk presented by M. Goodman at Neutrino 2002, "Other Atmospheric Neutrino Experiments".

[4] Probing CPT Violation with Atmospheric Neutrinos, S. Skadhauge, hep-ph0112189.

[5] Neutrinos as the Messenger of CPT Violation, G. Barenboim, L. Borissov, J. Lykken, A. Smirnov, Submitted to Phys.Rev.Let. hep-ph/0108199.

[6] CPT Violation and the Nature of Neutrinos, G. Barenboim, J. Beacom, L. Borissov, B. Kayser, hep-ph/0203261.

[7] Neutrinos that violate CPT and the Experiments That Love Them, G. Barenboim, L. Borissov, J. Lykken, hep-ph/0201080.

[8] Interpreting the LSND Anomaly: Sterile Neutrinos of CPT Violation or...?, A. Strumia, hep-ph/0201134.

[9] M. Shiozawa for the Super-Kamiokande Collaboration, Presented at Neutrino 2002, Munich.

[10] Atmospheric Neutrino Flux Above 1 GeV, V. Agrawal, T. Gaisser, P. Lipari, T. Stanev, Phys.Rev.D53 (1996) 1314.

[11] Study of the Atmospheric Neutrino Flux in the Multi-GeV Energy Range, The Superkamiokande Collaboration (Y. Fukuda etal.), Phys.Lett.B436 (1998) 33.

[12] Prototype Veto Shield Construction, W. Miller, April 2002, http://hep.caltech.edu/ michael/shield/vetocon.doc.

[13] Use of the Soudan 2 Shield in MINOS, The MINOS Collaboration, NuMI note 840, May 2002.